LIMIT CYCLE OSCILLATION CONTROL OF AEROELASTIC SYSTEM USING MODEL-ERROR CONTROL SYNTHESIS

Jongrae Kim*
Department of Electrical & Computer Engineering
University of California
Santa Barbara, CA, 93106-9560

John L. Crassidis†
Department of Mechanical & Aerospace Engineering
University at Buffalo, The State University of New York
Amherst, NY 14260-4400

ABSTRACT

Model-error control synthesis is a nonlinear robust control approach that uses an optimal solution to cancel the effects of modelling errors and external disturbances on a system. In this paper the optimal solution for a modified approximate receding-horizon problem is used to determine the model error in an aeroelastic system, which has several uncertain parameters, including a nonlinear spring constant. To verify the control performance the approach is applied to compensate the limit cycle oscillation of the system. Simulation results show the performance of the model-error control synthesis approach.

INTRODUCTION

Model-Error Control Synthesis (MECS) is a signal synthesis adaptive control method.[1] Robustness is achieved by applying a correction control, which is determined during the estimation process, to the nominal control vector thereby eliminating the effects of modelling errors at the system output.[2] The model-error vector is estimated by using either a one-step ahead prediction approach,[1,3] an Approximate Receding-Horizon (ARH) approach,[4] or a Modified Approximate Receding-Horizon (MARH) approach.[5] Choosing among the one-step ahead prediction approach, the ARH approach, or the MARH approach to determine the model error depends on the particular properties and required robustness in the system to be controlled.

In Ref. [1] MECS with the one-step ahead prediction approach is first applied to suppress the wing rock motion of a slender delta wing, which is described by a highly nonlinear differential equation. Results indicated that this approach provides adequate robustness for this particular system. In Ref. [3] a simple study to test the stability of the closed-loop system is presented using a Padé approximation for the time delay, which showed the relation between the system zeros and the weighting in the cost function. The analysis proved that some systems may not be stabilized using the original model-error estimation algorithm, which lead to the ARH approach in the MECS design to determine the model-error vector in the system.[4]

The closed-form solution of the ARH approach using Quadratic Programming (QP) is first presented by Lu.[6] The model-error vector is determined by the ARH optimal solution.[4] Using the ARH approach, the capability of MECS is expanded so that unstable non-minimum phase systems can be stabilized. Furthermore, Ref. [4] shows a method to calculate the stable regions with respect to the weighting and the length of receding-horizon step-time using the Hermite-Biehler theorem.[7] After the stable region is found, the weighting and the length of receding-horizon step-time are chosen to minimize the ∞-norm of the sensitivity function.[4]

The ARH solution for an r^{th}-order relative degree system shows that the model-error solution is zero before the end of receding-horizon step-time is reached. Some parts of the model-error vector are separated completely from the constraints, so that the optimal solution for those parts are automatically zero. To avoid this situation for all model-error elements of each constraint at the time before the end of receding-horizon step-time, the state prediction is substituted by an r^{th}-order Taylor series expansion instead of a repeated first-order expansion in the ARH approach. We call this the Modified Approximate Receding-Horizon (MARH) approach, which leads to an even more robust MECS law than with the ARH solution.[5]

In Ref. [5] the MARH approach is used to the spacecraft attitude control problem for the case where the only available information is attitude-angle measurements, i.e., with no angular-velocity measurements.

*Post-Doctoral Fellow, Member AIAA, jongrae@ece.ucsb.edu
†Associate Professor, Associate Fellow AIAA, johnc@eng.buffalo.edu

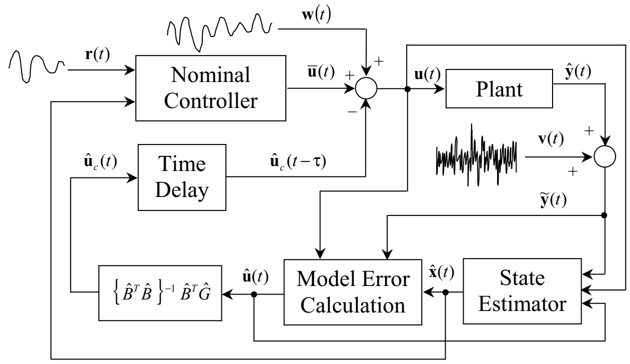

Fig. 1 Overall Block Diagram with MECS

In addition the relation between each optimization method and the damping coefficient in the simple mass-spring-damper system is shown in Ref. [8].

In this paper MECS is used to control an aeroelastic system, which has several uncertain parameters, including a nonlinear spring constant. In Ref. [9] to cancel the nonlinear parts and obtain the desired closed-loop dynamics a feedback linearization technique is used. In addition parameter uncertainties in the dynamics are compensated using an adaptive control scheme. Similar to the design steps for the spacecraft attitude maneuver problem in Ref. [5], we adopt the feedback linearization parts of the control in Ref. [9], but instead of the adaptive control parts, MECS will be designed to cancel the model uncertainties.

The organization of this paper is as follows. First, the MARH approach to estimate the model-error vector in a system is summarized. Second, the new approach is applied to the limit cycle compensation of the aeroelastic system. An optimal design scheme is presented to determine the weighting factor and receding-horizon time-length. Also, globally quadratic stability is provided for a norm bounded nonlinear uncertainty. Finally, the results are verified through the simulation.

MECS

The block diagram with MECS is shown in Fig. 1, where $\mathbf{r}(t)$ is the reference command. The model error is determined using the estimated states, $\hat{\mathbf{x}}(t)$, the control input, $\mathbf{u}(t)$, and the current measurement, $\tilde{\mathbf{y}}(t)$. The determined model error, $\hat{\mathbf{u}}(t)$, corrects not only the nominal control input, $\bar{\mathbf{u}}(t)$, but also the filter model. After the model error is determined, any state estimator or observer can be implemented, including a Kalman filter. The total control input $\mathbf{u}(t)$ with model-error correction is given by

$$\mathbf{u}(t) = \bar{\mathbf{u}}(t) - \hat{\mathbf{u}}_c(t-\tau) \tag{1}$$

where $\bar{\mathbf{u}}(t)$ is the nominal control input at time t, which can be any controller, i.e., Proportional-Integrate-Derivative (PID) Control, Lead-Lag Compensator, Sliding Mode Control, H_∞ Control, Linear Quadratic Regulator (LQR) Control, Linear Quadratic Gaussian (LQG) Control, etc. The time delay τ is always present in the overall MECS design because the measurement $\tilde{\mathbf{y}}(t)$ must be given before the error in the system can be corrected. The term $\hat{\mathbf{u}}_c\,(t-\tau)$ is used to cancel the estimated model error at time $t-\tau$, determined by the current information using a Pseudo-Inverse ($n \geq q_u$, i.e., under-actuated) as follows:

$$\hat{\mathbf{u}}_c(t) = [\hat{B}^T\,\hat{B}]^{-1}\,\hat{B}^T\,\hat{G}\,\hat{\mathbf{u}}(t) \tag{2}$$

When $\hat{B}\,[\hat{\mathbf{x}}(t)] = \hat{G}\,[\hat{\mathbf{x}}(t)]$, i.e., separate actuators are installed for each dynamics part, $\hat{\mathbf{u}}_c(t)$ is equal to $\hat{\mathbf{u}}(t)$, which will be the case for the spacecraft attitude control problem.

In this section the Modified Approximate Receding Horizon (MARH) approach to estimate the model-error vector, $\hat{\mathbf{u}}(t)$, in a system is summarized and the quadratic stability concept for providing nonlinear stability proof is introduced.

OPTIMAL MODEL ERROR SOLUTION

The receding-horizon optimization problem is set up as follows:[6]

$$\min_{\hat{\mathbf{u}}} J\,[\hat{\mathbf{x}}(t),\,t,\,\hat{\mathbf{u}}(t)] = \frac{1}{2}\int_t^{t+T} \left[\mathbf{e}^T(\xi)\,R^{-1}(\xi)\,\mathbf{e}(\xi) + \hat{\mathbf{u}}^T(\xi)\,W(\xi)\,\hat{\mathbf{u}}(\xi)\right] d\xi \tag{3}$$

subject to the following:

$$\dot{\hat{\mathbf{x}}}(t) = \hat{\mathbf{f}}\,[\hat{\mathbf{x}}(t)] + \hat{B}\,[\hat{\mathbf{x}}(t)]\,\mathbf{u}(t) + \hat{G}\,[\hat{\mathbf{x}}(t)]\,\hat{\mathbf{u}}(t) \tag{4a}$$
$$\hat{\mathbf{y}}(t) = \hat{\mathbf{c}}\,[\hat{\mathbf{x}}(t)] \tag{4b}$$

where $R^{-1}(\xi)$ and $W(\xi)$ are positive-definite and symmetric weighting matrices for all $\xi \in [t, t+T]$, $\hat{\mathbf{f}}\,[\hat{\mathbf{x}}(t)] \in \Re^n$ is the assumed model vector, $\hat{B}\,[\hat{\mathbf{x}}(t)] \in \Re^{n\times q_u}$ is the assumed control input distribution matrix, $\hat{G}\,[\hat{\mathbf{x}}(t)] \in \Re^{n\times q_w}$ is the model-error distribution matrix, $\hat{\mathbf{x}}(t) \in X \subset \Re^n$ is the state estimate vector, $\mathbf{u}(t) \in \Omega_u \subset \Re^{q_u}$ is the control input, $\hat{\mathbf{u}}(t) \in \Omega_{\hat{u}} \subset \Re^{q_w}$ is the to-be-determined model error, which also includes external disturbances, $\hat{\mathbf{c}}\,[\hat{\mathbf{x}}(t)] \in \Re^m$ is the measurement vector ($m \leq n$ in general), and $\hat{\mathbf{y}}(t) \in \Re^m$ is the estimated output vector.[6] Also, we assume that a unique solution for $\hat{\mathbf{x}}(t)$ exists, and $\mathbf{e}(t+T) = 0$ where the residual error is defined by

$$\mathbf{e}(t) = \tilde{\mathbf{y}}(t) - \hat{\mathbf{y}}(t) \tag{5}$$

where $\tilde{\mathbf{y}}(t)$ is the measurement. Note that T is the receding-horizon optimization-interval, which is not the sampling interval in general.

For most mechanical systems $\Omega_u \subset \Omega_{\hat{u}}$, i.e., the system is under-actuated or fully actuated at the maximum, so that $q_u \leq q_w$, where q_w is the dimension of the dynamics parts. The admissible sets X and

$\Omega_u \subset \Omega_{\hat{u}}$ are compact and $X \times \Omega_{\hat{u}}$ contains a neighborhood around the origin. One important assumption is $m \geq q_w$, i.e., the dimension of the measurement vector is at least the dimension of the dynamics. Also, we assume that the rank of $\hat{G}\left[\hat{\mathbf{x}}(t)\right]$ is q_w, i.e., full rank. In addition controllability, observability, stable zero dynamics, and well-defined relative degree with respect to $\hat{\mathbf{u}}(t)$ are presumed, and the assumptions about continuity and $\hat{\mathbf{f}}\left(\mathbf{0}\right) = \mathbf{0}$ hold. Finally, we assume that each element of the model-error vector affects the output.

State-observable measurements are assumed for Eq. (4b) in the following form:

$$\tilde{\mathbf{y}}(t) = \mathbf{c}[\mathbf{x}(t)] + \mathbf{v}(t) \tag{6}$$

where $\tilde{\mathbf{y}}(t) \in \Re^m$ is the measurement vector at time t, and $\mathbf{v}(t) \in \Re^m$ is the measurement noise vector, which is assumed to be a zero-mean, stationary, Gaussian noise distributed process with $E\left\{\mathbf{v}(t)\right\} = \mathbf{0}$ and $E\left\{\mathbf{v}(t)\,\mathbf{v}^T(t+\Delta t)\right\} = R_v\,\delta(\Delta t)$, where $E\{\cdot\}$ is expectation, $R_v \in \Re^{m\times m}$ is a positive-definite symmetric covariance matrix, $\delta(\cdot)$ is Dirac delta function, and Δt is the sampling rate for the discrete-time measurement case.

At each time t, the model-error solution $\hat{\mathbf{u}}$ over a finite horizon $[t,\, t+T]$ is determined on-line. Define $h \equiv T/N$ for some integer $N \geq n/m$, where N is the number of sub-intervals on $[t,\, t+T]$. In addition since the future values of $\tilde{\mathbf{y}}(t)$ and $\mathbf{u}(t)$ are unknown in general, $\tilde{\mathbf{y}}(t)$ and $\mathbf{u}(t)$ are assumed to remain constant over the finite horizon $[t,\, t{+}T]$. Now $\hat{\mathbf{y}}(t{+}kh)$ for each $k = 1,\, 2,\, \cdots,\, Nh = T$ is approximated. The output prediction at $t + (k+1)h$ is given by

$$\begin{aligned}
&\hat{\mathbf{y}}\left[t + (k+1)\,h\right] \approx \hat{\mathbf{y}}\left(t + kh\right) + \mathbf{z}\left[\hat{\mathbf{x}}\left(t+kh\right),\, h\right] \\
&\quad + \Lambda(h)\, S_u\left[\hat{\mathbf{x}}\left(t+kh\right)\right]\, \mathbf{u}(t) \\
&\quad + \Lambda(h)\, S_{\hat{u}}\left[\hat{\mathbf{x}}\left(t+kh\right)\right]\, \hat{\mathbf{u}}\left(t+kh\right)
\end{aligned} \tag{7}$$

for $k = 1,\, 2,\, \ldots,\, N$, where $\hat{\mathbf{y}}\left(t+kh\right)$ and $\hat{\mathbf{x}}\left(t+kh\right)$ are given by the predictions from the previous stage. This process is repeated up to all $\hat{\mathbf{x}}\left(t+kh\right)$ written in terms of $\hat{\mathbf{x}}\left(t\right)$. The i^{th} component of $\mathbf{z}\left[\hat{\mathbf{x}}(t),\, h\right]$ is given by

$$z_i\left[\hat{\mathbf{x}}(t),\, h\right] = \sum_{k=1}^{p_i} \frac{h^k}{k!}\; L_{\hat{\mathbf{f}}}^k(c_i) \tag{8}$$

where $L_{\hat{\mathbf{f}}}^k(c_i)$ is the k^{th} Lie derivative, defined by

$$L_{\hat{\mathbf{f}}}^0(c_i) = c_i \tag{9a}$$

$$L_{\hat{\mathbf{f}}}^k(c_i) = \left[\frac{\partial L_{\hat{\mathbf{f}}}^{k-1}(c_i)}{\partial \hat{\mathbf{x}}}\right]^T \hat{\mathbf{f}}, \quad \text{for } k \geq 1 \tag{9b}$$

where the gradient is represented by a column vector with elements $\left(\partial c_i/\partial \mathbf{x}\right)_k = \partial c_i/\partial x_k$. The i^{th} rows of $S_u\left[\hat{\mathbf{x}}(t)\right]$ and $S_{\hat{u}}\left[\hat{\mathbf{x}}(t)\right]$ are given by

$$\mathbf{s}_{u_i} = \left\{L_{\hat{\mathbf{b}}_1}\left[L_{\hat{\mathbf{f}}}^{p_i-1}(c_i)\right],\, \cdots,\, L_{\hat{\mathbf{b}}_{q_u}}\left[L_{\hat{\mathbf{f}}}^{p_i-1}(c_i)\right]\right\} \tag{10a}$$

$$\mathbf{s}_{\hat{u}_i} = \left\{L_{\hat{\mathbf{g}}_1}\left[L_{\hat{\mathbf{f}}}^{p_i-1}(c_i)\right],\, \cdots,\, L_{\hat{\mathbf{g}}_{q_w}}\left[L_{\hat{\mathbf{f}}}^{p_i-1}(c_i)\right]\right\} \tag{10b}$$

for $i = 1,\, 2,\, \ldots,\, m$, where $\hat{\mathbf{b}}_j$ is the j^{th} column of $\hat{B}\left[\hat{\mathbf{x}}(t)\right]$, $\hat{\mathbf{g}}_j$ is the j^{th} column of $\hat{G}\left[\hat{\mathbf{x}}(t)\right]$, and the Lie derivative in Eq. (10) is defined by

$$L_{\hat{\mathbf{b}}_j}\left[L_{\hat{\mathbf{f}}}^{p_i-1}(c_i)\right] \equiv \left[\frac{\partial L_{\hat{\mathbf{f}}}^{p_i-1}(c_i)}{\partial \hat{\mathbf{x}}}\right]^T \hat{\mathbf{b}}_j \tag{11}$$

for $j = 1,\, 2,\, \ldots,\, q_u$, and

$$L_{\hat{\mathbf{g}}_j}\left[L_{\hat{\mathbf{f}}}^{p_i-1}(c_i)\right] \equiv \left[\frac{\partial L_{\hat{\mathbf{f}}}^{p_i-1}(c_i)}{\partial \hat{\mathbf{x}}}\right]^T \hat{\mathbf{g}}_j \tag{12}$$

for $j = 1,\, 2,\, \ldots,\, q_w$.

Define the following:

$$\begin{aligned}
L(k\,h) \equiv\; &\mathbf{e}^T(t+k\,h) R_k^{-1} \mathbf{e}(t+k\,h) \\
&+ \hat{\mathbf{u}}^T(t+k\,h)\, W_k\, \hat{\mathbf{u}}(t+k\,h)
\end{aligned} \tag{13}$$

The cost function to be minimized is approximated using a trapezoidal formula or Simpson's rule as follows:[6] when N is odd,

$$\bar{J} = \frac{h}{2}\sum_{k=1}^{N}\left\{\frac{1}{2}\,L\left[(k-1)\,h\right] + \frac{1}{2}\,L\left(kh\right)\right\} \tag{14}$$

when N is even,

$$\begin{aligned}
\bar{J} = \frac{h}{6}\sum_{k=0}^{(N/2)-1} &\left\{L\left(2kh\right) + 4L\left[(2k+1)\,h\right]\right. \\
&\left. + L\left[2\left(k+1\right)h\right]\right\}
\end{aligned} \tag{15}$$

With the following definition:

$$\boldsymbol{\nu}_0 \equiv \left\{\hat{\mathbf{u}}^T(t),\;\; \hat{\mathbf{u}}^T(t+h),\;\; \cdots,\;\; \hat{\mathbf{u}}^T[t+(N-1)h]\right\}^T \tag{16}$$

The approximate cost, $\bar{J}$, can be rewritten in quadratic form as

$$\bar{J} = \frac{1}{2}\,\boldsymbol{\nu}_0^T H_0\, \boldsymbol{\nu}_0 + \mathbf{g}_0^T(\hat{\mathbf{x}}, \mathbf{u}, \tilde{\mathbf{y}})\, \boldsymbol{\nu}_0 + q_0(\hat{\mathbf{x}}, \mathbf{u}, \tilde{\mathbf{y}}) \tag{17}$$

where H_0, $\mathbf{g}_0$ and q_0 are functions of $L(k\,h)$.[6] Also, the terminal constraint, $\mathbf{e}(t+T) = 0$, can be formulated as a constraint on $\boldsymbol{\nu}_0$ as follows:

$$M^T \boldsymbol{\nu}_0 = \mathbf{d}(t) \tag{18}$$

Finally, the solution of the QP problem is given by

$$\boldsymbol{\nu}_0 = -\left[H_0^{-1} - H_0^{-1} M \left(M^T H_0^{-1} M\right)^{-1} M^T H_0^{-1}\right] \mathbf{g}_0(t) + \left[H_0^{-1} M \left(M^T H_0^{-1} M\right)^{-1}\right] \mathbf{d}(t) \tag{19}$$

where the rank of M is m. The first q_w equations give a current model error minimizing the cost function, which leads to a predictive filter structure:

$$\hat{\mathbf{u}}[t;\, \hat{\mathbf{x}}(t),\, \mathbf{u}(t),\, \tilde{\mathbf{y}}(t),\, h] = I_{q_w \times N}\ \boldsymbol{\nu}_0 \tag{20}$$

where $I_{q_w \times N}$ is a $\min(q_w, N) \times \min(q_w, N)$ identity matrix with zeros for the remaining elements.

QUADRATIC STABILITY

To provide a stability proof for nonlinear systems, the following are summarized from Ref. [10]:

Definition 1 *Quadratically Stable*
Consider the following system with nonlinear uncertainty $\Delta\mathbf{f}[\mathbf{x}(t)]$*:*

$$\dot{\mathbf{x}}(t) = A\,\mathbf{x}(t) + \Delta\mathbf{f}[\mathbf{x}(t)] \tag{21}$$

where $\mathbf{x}(t) \in \Re^n$ *and the nonlinear uncertainty* $\Delta\mathbf{f}[\mathbf{x}(t)] \equiv E_f\,\boldsymbol{\delta}[\mathbf{x}(t)]$ *is a* C^0 *function, and* $\boldsymbol{\delta}[\mathbf{x}(t)]$ *is a element of the following set:*

$$\Omega \equiv \{\, \boldsymbol{\delta}[\mathbf{x}(t)] \mid \|\boldsymbol{\delta}[\mathbf{x}(t)]\|_\infty \le \|N_f\,\mathbf{x}(t)\|_\infty,\ \forall\ \mathbf{x}(t)\} \tag{22}$$

where E_f *and* N_f *are some constant matrices. The system, Eq. (21), is said to be quadratically stable if there exists a positive-definite symmetric matrix* $P_q > 0$ *such that*

$$\{A\mathbf{x}(t) + \Delta\mathbf{f}[\mathbf{x}(t)]\}^T\ P_q\,\mathbf{x}(t) + \mathbf{x}^T(t)\,P_q\ \{A\mathbf{x}(t) + \Delta\mathbf{f}[\mathbf{x}(t)]\} < 0 \tag{23}$$

for all nonzero $\mathbf{x}(t) \in \Re^n$ *and all admissible nonlinear uncertainty,* $\Delta\mathbf{f}[\mathbf{x}(t)]$. ■

Definition 2 *Quadratic Cost Matrix,* P_q
A positive definite matrix $P_q > 0$ *is said to be a quadratic cost matrix for Eq. (21) and the following cost function:*

$$J_q = \int_0^\infty \mathbf{x}^T(t)\,Q_q\,\mathbf{x}(t)\,dt \tag{24}$$

where $Q_q \ge 0$*, if*

$$\{A\mathbf{x}(t) + \Delta\mathbf{f}[\mathbf{x}(t)]\}^T\ P_q\,\mathbf{x}(t) + \mathbf{x}^T(t)\,P_q\ \{A\mathbf{x}(t) + \Delta\mathbf{f}[\mathbf{x}(t)]\} < -\mathbf{x}^T(t)\,Q_q\,\mathbf{x}(t) \tag{25}$$

for all nonzero $\mathbf{x}(t) \in \Re^n$ *and all admissible nonlinear uncertainty,* $\Delta\mathbf{f}[\mathbf{x}(t)]$. ■

Theorem 1 *The Cost Function Bound*
If $P_q > 0$ *is a quadratic cost matrix of Eq. (21), then the cost function is bounded by*

$$J_q \le \mathbf{x}^T(0)\,P_q\,\mathbf{x}(0) \tag{26}$$

and if the system is quadratically stable, then there exists a quadratic cost matrix. ■

Lemma 1 H_∞ *Norm Bound Condition*

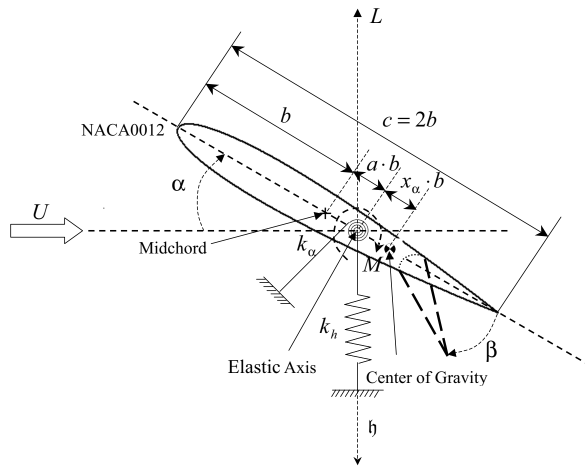

Fig. 2 Aeroelastic System

For the system, Eq. (21), there exists a quadratic cost matrix, $P_q > 0$*, if and only if the following conditions hold:*

1. *A is a stable matrix.*
2. *The following* H_∞ *norm bound is satisfied for some* $\epsilon > 0$*:*

$$\left\| \begin{bmatrix} N_f \\ \sqrt{\epsilon}\,Q_q \end{bmatrix} (s\,I_n - A)^{-1}\ E_f \right\|_\infty < 1 \tag{27}$$

Then, for such ϵ*, the Riccati equation*

$$A^T P_q + P_q\,A + \epsilon\,P_q\,E_f\,E_f^T\,P_q + \frac{1}{\epsilon}\,N_f^T\,N_f = -Q_q \tag{28}$$

has a solution. ■

AEROELASTIC SYSTEM

In this section the MECS design will be applied to the control of limit cycle oscillations of the aeroelastic system shown in Fig. 2. The aeroelastic system has two degrees of freedom, i.e., pitch angle, α, and plunge displacement, $\mathfrak{h}$, which are measured by US Digital E2 digital optical encoders.[9]

PROBLEM FORMULATION

The equations of motion for the system shown in Fig. 2 are given by

$$\begin{bmatrix} m_T & m_W\,x_\alpha\,b \\ m_W\,x_\alpha\,b & I_\alpha \end{bmatrix} \begin{Bmatrix} \ddot{\mathfrak{h}} \\ \ddot{\alpha} \end{Bmatrix} + \begin{bmatrix} c_h & 0 \\ 0 & c_\alpha \end{bmatrix} \begin{Bmatrix} \dot{\mathfrak{h}} \\ \dot{\alpha} \end{Bmatrix} + \begin{bmatrix} k_h & 0 \\ 0 & k_\alpha(\alpha) \end{bmatrix} \begin{Bmatrix} \mathfrak{h} \\ \alpha \end{Bmatrix} = \begin{Bmatrix} -L \\ M \end{Bmatrix} \tag{29}$$

where m_T is the total mass, m_W is the mass of the wing only, and I_α is the moment of inertia about the elastic axis. The terms a and x_α are non-dimensionalized elastic axis and center of mass locations by the length of midchord, b, respectively. The terms c_h and c_α are plunge and pitch structural damping coefficients, and the structural stiffness for plunge and pitch motions are k_h and k_α, respectively.

The term $k_\alpha(\alpha)$ is a nonlinear function of pitch angle as follows:[9]

$$k_\alpha(\alpha) = \sum_{i=0}^{\infty} k_{\alpha i}\, \alpha^i \tag{30}$$

where the $k_{\alpha i}$'s are constants. For numerical simulation purposes, the following 4^{th}-order approximation is used as the real value of $k_\alpha(\alpha)$:[9]

$$\begin{aligned} k_\alpha(\alpha) &= 6.833 + 9.997\alpha + 667.685\alpha^2 \\ &\quad + 26.569\alpha^3 - 5087.931\alpha^4 \quad [\text{N·m/rad}] \end{aligned} \tag{31}$$

As shown in Ref. [9], the above approximation well matches the experimental results within $\pm 11.49°$ of α. In addition the following quasi-steady aerodynamic model for the lift, L, and the moment, M are used:[9]

$$\begin{aligned} L &= \rho U^2 b\, c_{l\alpha} \left[\alpha + \frac{\dot{\mathfrak{h}}}{U} + \left(\frac{1}{2} - a\right) \frac{b\,\dot\alpha}{U}\right] \\ &\quad + \rho U^2 b\, c_{l\beta}\, \beta \end{aligned} \tag{32a}$$

$$\begin{aligned} M &= \rho U^2 b^2 c_{m\alpha} \left[\alpha + \frac{\dot{\mathfrak{h}}}{U} + \left(\frac{1}{2} - a\right) \frac{b\,\dot\alpha}{U}\right] \\ &\quad + \rho U^2 b^2 c_{m\beta}\, \beta \end{aligned} \tag{32b}$$

where ρ is air density, U is the freestream velocity, $c_{l\alpha}$ and $c_{m\alpha}$ are the aerodynamic lift and moment coefficients, respectively, and β is the flap defection.

Define the following:

$$\phi_1 \equiv \alpha,\ \ \phi_2 \equiv \dot\alpha,\ \ \phi_3 \equiv \mathfrak{h},\ \ \phi_4 \equiv -g_3\,\dot\alpha + g_4\,\dot{\mathfrak{h}} \tag{33}$$

The state-space form of Eq. (29) is given by

$$\dot\phi_1(t) = \phi_2(t) \tag{34a}$$

$$\begin{aligned} \dot\phi_2(t) &= \Big\{-P_U[\phi_1(t)]\,\phi_1(t) - [c_4 + c_3\,A_{32}]\ \phi_2(t) \\ &\qquad -k_3\,\phi_3(t) - \frac{c_3}{g_4}\,\phi_4(t)\Big\} + g_4\,U^2\,\beta(t) \\ &\equiv f_1[\boldsymbol{\phi}(t)] + g_4\,U^2\,\beta(t) \end{aligned} \tag{34b}$$

$$\dot\phi_3(t) = A_{32}\,\phi_2(t) + A_{34}\,\phi_3(t) \tag{34c}$$

$$\begin{aligned} \dot\phi_4(t) &= \{g_3\,P_U[\phi_1(t)] - g_4\,Q_U[\phi_1(t)]\}\ \phi_1(t) \\ &\quad + A_{42}\,\phi_2(t) + A_{43}\,\phi_3(t) + A_{44}\,\phi_4(t) \\ &\equiv f_2[\phi_1(t)]\,\phi_1(t) \\ &\quad + A_{42}\,\phi_2(t) + A_{43}\,\phi_3(t) + A_{44}\,\phi_4(t) \end{aligned} \tag{34d}$$

where the definition of each parameter in the above is given in the Appendix A. In compact form the state-space representation is given by

$$\dot{\boldsymbol{\phi}}(t) \equiv \mathbf{f}(U,\, a,\, k_\alpha) + B(a)\,\beta(t) \tag{35a}$$

$$\mathbf{y}(t) = \begin{Bmatrix}\alpha(t) \\ \mathfrak{h}(t)\end{Bmatrix} = C\,\boldsymbol{\phi}(t) \tag{35b}$$

where

$$\boldsymbol{\phi}(t) \equiv \begin{Bmatrix}\phi_1(t) & \phi_2(t) & \phi_3(t) & \phi_4(t)\end{Bmatrix}^T \tag{36a}$$

$$\mathbf{f}(U,\, a,\, k_\alpha) \equiv$$

$$\begin{Bmatrix} \phi_2(t) \\ f_1[\phi_1(t)] \\ A_{32}\,\phi_2(t) + A_{34}\,\phi_4(t) \\ f_2[\phi_1(t)]\,\phi_1(t) + A_{42}\,\phi_2(t) + A_{43}\,\phi_3(t) + A_{44}\,\phi_4(t) \end{Bmatrix} \tag{36b}$$

$$B(a) \equiv \begin{Bmatrix}0 & g_4\,U^2 & 0 & 0\end{Bmatrix}^T \tag{36c}$$

$$C \equiv \begin{bmatrix}1 & 0 & 0 & 0 \\ 0 & 0 & 1 & 0\end{bmatrix} \tag{36d}$$

For simplicity it is assumed that the uncertainty in the dynamics occurs from the velocity, U, the location of elastic axis, a, which has the significant role in the stability, and the nonlinear torsional spring constant, k_α. The measurement is given by

$$\tilde{\mathbf{y}}(t) = C\,\boldsymbol{\phi}(t) + \mathbf{v}(t) \tag{37}$$

where $\mathbf{v}(t) \in \Re^2$, $E\{\mathbf{v}(t)\} = \mathbf{0}$ and

$$E\left\{\mathbf{v}(t)\,\mathbf{v}^T(t + \Delta t)\right\} = \begin{bmatrix} r_\alpha & 0 \\ 0 & r_h \end{bmatrix}\ \delta(\Delta t) \tag{38}$$

The model-error representation of the state-space form is as follows:

$$\dot{\hat{\boldsymbol{\phi}}}(t) = \hat{\mathbf{f}}(\hat U,\, \hat a,\, \hat k_\alpha) + \hat B(\hat U,\, \hat a)\,\beta(t) + \hat G\,\hat{\mathbf{u}}(t) \tag{39}$$

where $\hat U$ and $\hat a$ are the nominal values of U and a, respectively. The nominal value of $k_\alpha(\alpha)$ is given by

$$\hat k_\alpha = 6.833 \quad [\text{N·m/rad}] \tag{40}$$

i.e., only the linear part in the resulting moment by the torsional spring with respect to α is assumed:

$$\hat G \equiv \begin{bmatrix} 0 & 0 & 0 \\ 1 & 0 & 0 \\ 0 & 1 & 0 \\ 0 & 0 & 1 \end{bmatrix} \tag{41}$$

and the model-error, $\hat{\mathbf{u}}(t) = \{\hat u_1(t),\, \hat u_2(t),\, \hat u_3(t)\}^T$, is to be determined.

NOMINAL CONTROLLER DESIGN

We summarize the nominal controller design using feedback linearization in Ref. [9]. The system is given by

$$\dot{\hat{\boldsymbol{\phi}}}(t) = \hat{\mathbf{f}}(\hat U,\, \hat a,\, \hat k_\alpha) + \hat B(\hat U,\, \hat a)\,\beta(t) + \hat G\,\hat{\mathbf{u}}(t) \tag{42}$$

The partial feedback linearization control input is given by

$$\beta(t) = \frac{\left\{ -F[\hat{\boldsymbol{\phi}}(t)] + \dfrac{m_T\,\hat{k}_\alpha}{\hat{d}}\,\hat{\phi}_1(t) + \bar{\nu}(t) - \hat{\nu}(t-\tau) \right\}}{\hat{g}_4\,\hat{U}^2} \tag{43}$$

where

$$F[\hat{\boldsymbol{\phi}}(t)] \equiv -\hat{k}_4\,\hat{U}^2\,\hat{\phi}_1(t) - \left[\hat{c}_4 + \hat{c}_3\,\frac{\hat{g}_3}{\hat{g}_4}\right]\,\hat{\phi}_2(t) - \hat{k}_3\,\hat{\phi}_3(t) - \frac{\hat{c}_3}{\hat{g}_4}\,\hat{\phi}_4(t) \tag{44a}$$

$$\bar{\nu}(t) \equiv -\bar{k}_1\,\hat{\phi}_1(t) - \bar{k}_2\,\hat{\phi}_2(t) \tag{44b}$$

Also, $\hat{\nu}(t-\tau)$ is the to-be-determined model-error correction and $\hat{\mathfrak{f}} = \mathfrak{f}(\hat{U},\,\hat{a},\,\hat{k}_\alpha)$, i.e., a function value with the nominal values. Then, the closed-loop dynamics is given by

$$\begin{Bmatrix} \dot{\hat{\phi}}_1(t) \\ \dot{\hat{\phi}}_2(t) \end{Bmatrix} = \begin{bmatrix} 0 & 1 \\ -\bar{k}_1 & -\bar{k}_2 \end{bmatrix} \begin{Bmatrix} \hat{\phi}_1(t) \\ \hat{\phi}_2(t) \end{Bmatrix} - \begin{Bmatrix} 0 \\ 1 \end{Bmatrix} \hat{\nu}(t-\tau) + \begin{Bmatrix} 0 \\ 1 \end{Bmatrix} \hat{u}_1(t) \tag{45}$$

In Ref. [9] an adaptive control part is designed so that $\hat{u}_1(t)$ approaches zero as time increases. Similar to the spacecraft attitude maneuver we will determine the model-error to minimize a cost function so that the model-error effects will vanish through the correction flap deflection, namely, $-\hat{\nu}(t-\tau)/(\hat{g}_4\,\hat{U}^2)$.

Let us consider the resulting zero dynamics, which are given by

$$\begin{aligned} \begin{Bmatrix} \dot{\hat{\phi}}_3(t) \\ \dot{\hat{\phi}}_4(t) \end{Bmatrix} &= \begin{bmatrix} 0 & \hat{A}_{34}(\hat{U},\,\hat{a}) \\ \hat{A}_{43}(\hat{U},\,\hat{a}) & \hat{A}_{44}(\hat{U},\,\hat{a}) \end{bmatrix} \begin{Bmatrix} \hat{\phi}_3(t) \\ \hat{\phi}_4(t) \end{Bmatrix} + \begin{Bmatrix} \hat{u}_2(t) \\ \hat{u}_3(t) \end{Bmatrix} \\ &= \begin{bmatrix} 0 & A_{34}(U,\,a) \\ A_{43}(U,\,a) & A_{44}(U,\,a) \end{bmatrix} \begin{Bmatrix} \hat{\phi}_3(t) \\ \hat{\phi}_4(t) \end{Bmatrix} \end{aligned} \tag{46}$$

The above zero dynamics are Hurwitz stable in the range of $-1 \le a \le 1$ and $0 < U \le 30$ [m/sec] as shown in Ref. [9]. Therefore, the main concern to cancel the model-error effects are given by Eq. (45) from a control point of view.

MODEL ERROR ESTIMATION

The model-error for the state estimator and control input correction will be determined. The nominal values are given by Table 1, which are the experiment setup by the Aeroelastic Group in Department of Aerospace Engineering, Texas A&M University at College Station, TX (the experimental data and the physical parameters are used with the permission by Dr. T. Strganac, who is the director of the Aeroelastic Group). The span of this wing model is 0.6 m. First, the Predictive filter will be designed and verified by the experimental data. Second, to cancel the model-error effects in Eq. (45) through the flap angle deflection, the optimal correction will be determined. Finally, the closed-loop response will be shown by simulation.

Table 1 Aeroelastic System Parameters

Parameters	Values
m_T	12.3870 [kg]
m_W	2.0490 [kg]
b (without flap)	0.1064 [m]
ρ	1.225 [kg/m^3]
a	$\hat{a}$ = -0.6
x_α	$[0.0873 - (b + a\cdot b)]\,/b$ [m]
I_α	$m_W\,x_\alpha^2\,b^2 + 0.0517$ [kg·m^2]
k_h	2844.4 [N/m]
$c_{l\alpha}$	6.28
$c_{l\beta}$	3.358
$c_{m\alpha}$	$(0.5 + a)\,c_{l\alpha}$
$c_{m\beta}$	-1.94
c_h	27.43 [kg/sec]
c_α	0.036 [kg·m^2/sec]

MODEL ERROR FOR STATE ESTIMATOR

With the nominal values given in Table 1, the state-space form of the model is obtained as follows:

$$\dot{\hat{\boldsymbol{\phi}}}(t) = \hat{A}\hat{\boldsymbol{\phi}}(t) + \hat{B}\,\beta(t) + \hat{G}_s\,\hat{\mathbf{u}}_s(t) \tag{47}$$

where each matrix is given in the Appendix A.

Since we have a measurement of $\mathfrak{h}$, the model-error, $\hat{u}_2(t)$, can be compensated by using a simple estimator such as a Luenberger observer or a Kalman filter, where $\hat{u}_2(t)$ is negligible.

Using the MARH approach with the following values:

$$N = 2, \quad h = 0.006 \text{ [sec]} \tag{48a}$$

$$r_{0h} = r_{0\alpha} = 1\times 10^{-6}, \quad r_p = 1 \tag{48b}$$

$$w_{0h} = w_{0\alpha} = 0.1, \quad w_p = 1 \tag{48c}$$

the model-error is determined by

$$\hat{u}_1(t) = -18008.7\,\hat{\phi}_1(t) - 217.5\,\hat{\phi}_2 - 810.2\,\hat{\phi}_3 + 14.7\,\hat{\phi}_4 + 136.2\,\beta(t) + 18218.8\,\tilde{\alpha}(t) + 227.3\,\tilde{\mathfrak{h}}(t) \tag{49a}$$

$$\hat{u}_3(t) = -1038.5\,\hat{\phi}_1(t) + 15.0\,\hat{\phi}_2 + 28595.7\,\hat{\phi}_3 - 845.1\,\hat{\phi}_4 - 0.5825\,\beta(t) + 1035.8\,\tilde{\alpha}(t) - 28759.3\,\tilde{\mathfrak{h}}(t) \tag{49b}$$

where Eqs. (49a) and (49b) are substituted into Eq. (47) with $\hat{U}$ = 16 m/sec. Since the measurement sampling time is 0.002 sec, the discrete form of the estimator with zero-order hold is given by[11]

$$\hat{\boldsymbol{\phi}}(k+1) = \hat{A}_d\,\hat{\boldsymbol{\phi}}(k) + \hat{B}_d\,\beta(k) + G_{y_k}\,\tilde{y}(k) \tag{50}$$

where each matrix is given in the Appendix A.

The above estimator is tested for 24 sets of the experimental data shown in Table 2. To compare the estimates we have to estimate $\dot{\hat{\alpha}}(t)$ and $\dot{\hat{\mathfrak{h}}}(t)$ using the whole measurement information including the acceleration measurements, i.e., $\ddot{\tilde{\alpha}}(t)$ and $\ddot{\tilde{\mathfrak{h}}}(t)$. Toward this end the following models are used:

$$\begin{Bmatrix} \dot{\hat{\alpha}}(t) \\ \ddot{\hat{\alpha}}(t) \\ \dddot{\hat{\alpha}}(t) \\ \dot{b}_\alpha(t) \end{Bmatrix} = \begin{bmatrix} 0 & 1 & 0 & 0 \\ 0 & 0 & 1 & 0 \\ 0 & 0 & 0 & 1 \\ 0 & 0 & 0 & 0 \end{bmatrix} \begin{Bmatrix} \hat{\alpha}(t) \\ \dot{\hat{\alpha}}(t) \\ \ddot{\hat{\alpha}}(t) \\ b_\alpha(t) \end{Bmatrix} + \begin{Bmatrix} 0 \\ 0 \\ 0 \\ 1 \end{Bmatrix} w_\alpha(t) \tag{51a}$$

$$\begin{Bmatrix} \dot{\hat{\mathfrak{h}}}(t) \\ \ddot{\hat{\mathfrak{h}}}(t) \\ \dddot{\hat{\mathfrak{h}}}(t) \\ \dot{b}_h(t) \end{Bmatrix} = \begin{bmatrix} 0 & 1 & 0 & 0 \\ 0 & 0 & 1 & 0 \\ 0 & 0 & 0 & 1 \\ 0 & 0 & 0 & 0 \end{bmatrix} \begin{Bmatrix} \hat{\mathfrak{h}}(t) \\ \dot{\hat{\mathfrak{h}}}(t) \\ \ddot{\hat{\mathfrak{h}}}(t) \\ b_h(t) \end{Bmatrix} + \begin{Bmatrix} 0 \\ 0 \\ 0 \\ 1 \end{Bmatrix} w_h(t) \tag{51b}$$

where b_α and b_h are the biases in the acceleration measurements, which are given by random walk models through w_α and w_h, which are zero-mean Gaussian white noise, respectively. The measurement equation is given by

Table 2 Aeroelastic System Experiment Cases

Experiment #	a	U [m/sec]	Flutter
1 ⇒ 5	-0.4	4, 6, 8, 10, 12	No
6 ⇒ 10	-0.4	14, 16, 18, 20, 22	Yes
11	-0.4	13 ⇒ 22	Yes
12	-0.4	22 ⇒ 13	Yes
13 ⇒ 17	-0.6	4, 6, 8, 10, 12	No
18 ⇒ 22	-0.6	14, 16, 18, 20, 22	Yes
23	-0.6	13 ⇒ 22	Yes
24	-0.6	22 ⇒ 13	Yes

$$\begin{Bmatrix} \tilde{\alpha}(t) \\ \ddot{\tilde{\alpha}}(t) \end{Bmatrix} = \begin{Bmatrix} \hat{\alpha}(t) \\ \ddot{\hat{\alpha}}(t) + b_\alpha(t) \end{Bmatrix} + \begin{Bmatrix} v_\alpha \\ v_{\ddot{\alpha}} \end{Bmatrix} \tag{52a}$$

$$\begin{Bmatrix} \tilde{\mathfrak{h}}(t) \\ \ddot{\tilde{\mathfrak{h}}}(t) \end{Bmatrix} = \begin{Bmatrix} \hat{\mathfrak{h}}(t) \\ \ddot{\hat{\mathfrak{h}}}(t) + b_h(t) \end{Bmatrix} + \begin{Bmatrix} v_h \\ v_{\ddot{h}} \end{Bmatrix} \tag{52b}$$

After transforming to discrete form with the sampling rate, 0.002 sec, and using the Rauch-Tung-Striebel (RTS) smoother, we can obtain accurate velocity estimates. The RTS smoother provides optimal estimates through an optimal combination of the forward and the backward Kalman filter.[12,13] Based on the velocity estimates from the RTS smoother the performance of the Predictive filter will be evaluated.

The absolute values of the mean of the errors between the estimate by the Predictive filter and the RTS smoother are shown in Figs. 3 and 4. As shown in the figures, the mean values of the pitch angle and the plunge displacement estimation errors are less than 0.23 arcsec and 0.19μm. The absolute values of

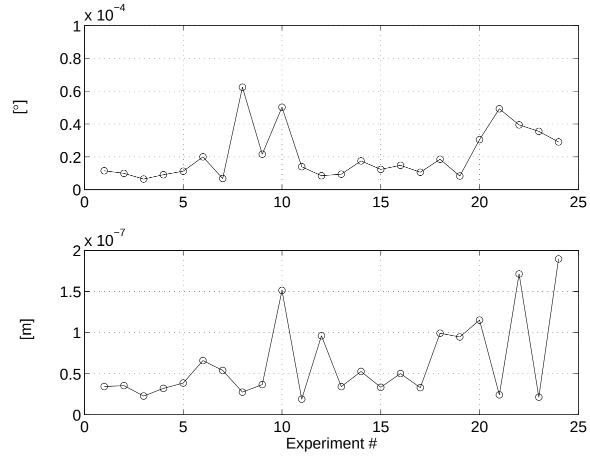

Fig. 3 Absolute Values of $\hat{\alpha}(t)$ and $\hat{\mathfrak{h}}(t)$ Estimation Error Mean

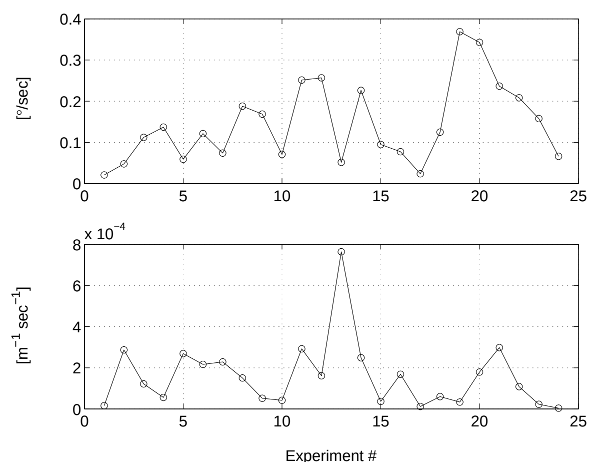

Fig. 4 Absolute Values of $\dot{\hat{\alpha}}(t)$ and $\dot{\hat{\phi}}_4(t)$ Estimation Error Mean

the mean for the $\dot{\hat{\alpha}}(t)$ and $\dot{\hat{\phi}}_4(t)$ are 0.37°/sec and $0.77{\times}10^{-3}$/(m·sec), respectively. As a result the Predictive filter, Eq. (50), estimates $\dot{\hat{\alpha}}(t)$ and $\dot{\hat{\phi}}_4(t)$ with small estimation errors in the sense of the estimates by RTS smoother for all the cases in Table 2. The time histories of $\dot{\hat{\alpha}}(t)$ for experiment #19 and $\dot{\hat{\phi}}_4(t)$ for experiment #13, which are the largest mean error cases by the Predictive filter are shown in Fig. 5. As shown in the figure, the Predictive filter yields accurate performance results, compared the RTS smoother results.

Since the midchord length, b, with flap is given by 0.135 m, each matrix used in the Predictive filter is as

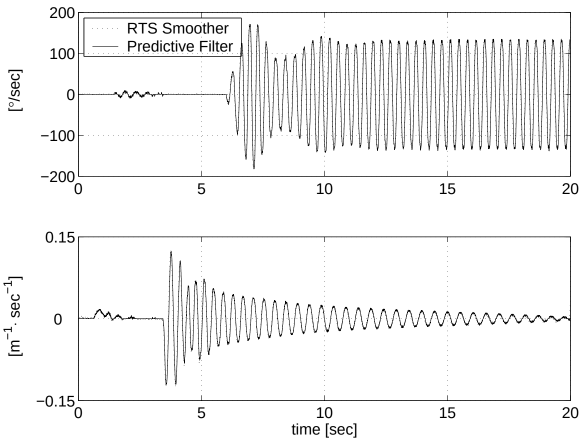

Fig. 5 Time History of the Estimated $\dot{\alpha}(t)$ for #19 and $\dot{\hat{\phi}}_4(t)$ for #13

follows:

$$\hat{A}_d \equiv \begin{bmatrix} 0.97 & 0.0016 & -0.0005 & 0.0000 \\ -29.1 & 0.62 & -0.39 & 0.0046 \\ 0.0005 & 0.0001 & 0.94 & -0.0017 \\ -1.44 & 0.0071 & 35.87 & 0.33 \end{bmatrix} \tag{53a}$$

$$\hat{B}_d \equiv \begin{Bmatrix} 0.0001 \\ 0.0897 \\ 0.0000 \\ 0.0045 \end{Bmatrix} \tag{53b}$$

$$G_{y_k} \equiv \begin{bmatrix} 0.0315 & 0.0003 \\ 29.1867 & 0.1996 \\ -0.0005 & 0.0592 \\ 1.4492 & -35.7531 \end{bmatrix} \tag{53c}$$

From now on, the above matrices will be used in the Predictive filter for the closed-loop control simulation.

MODEL ERROR FOR CONTROL INPUT

We can use Eq. (49a) as the correction control input to cancel the model-error effects. However, since the weights and h are selected so that the estimation error is as small as possible, the model-error correction from Eq. (49a) may not suitable as the control correction because it may saturate the flap deflection or the rate limit of the actuator. In this example the actuator constraints are given by

$$-12^\circ \le \beta(t) \le 12^\circ \tag{54a}$$

$$-150^\circ/\text{sec} \le \dot{\beta}(t) \le 150^\circ/\text{sec} \tag{54b}$$

From Eq. (45) with $\bar{k}_1 = 4$ and $\bar{k}_2 = 1.2$, the damping ratio of the model is $\zeta = 0.3 < 0.707$ and $\chi = \zeta\left(\sqrt{4\zeta^2+6} - 2\zeta\right) \approx 0.566 < 1$ (more details about χ can be found in Ref. [8]). Therefore, the MARH optimization method will be better than ARH approach. In addition the model-error correction of MARH with $N = 2$ is given in the Appendix B with the following definition:

$$\omega_n = \sqrt{\bar{k}_1}, \quad \zeta = \frac{\bar{k}_2}{2\sqrt{\bar{k}_1}} \tag{55}$$

Then, the model-error correction input is given by

$$\hat{\nu}(t) = a_1\,\hat{\phi}(t) + a_2\,\dot{\hat{\phi}}(t) - a_3\,\hat{\nu}(t-\tau) + a_4\,\tilde{\alpha}(t) \tag{56}$$

where each of the a_i's will be determined in the next section.

OPTIMAL DESIGN

From the Hermite-Biehler theorem the following is deduced:

Corollary 1 *Graphical interpretation for a 6^{th}-order Polynomial*
Consider the following 6^{th}-order polynomial:

$$d_{cl}(s) = c_6\,s^6 + c_5\,s^5 + c_4\,s^4 + c_3\,s^3 + c_2\,s^2 + c_1\,s + c_0 \tag{57}$$

where $c_6 > 0$, then $d_{cl}(s)$ is Hurwitz stable if and only if the stability index,

$$\varepsilon \equiv \mathrm{sc}(\kappa) \tag{58}$$

is greater than zero, where

$$\kappa \equiv \min\left(\text{I},\ \text{II-a},\ \text{II-b},\ \text{II-c},\ \text{III-a},\ \text{III-b},\ \text{III-c},\ \text{III-d}\right) \tag{59}$$

and

$$\text{I}:\ \underline{c}_0 > 0 \tag{60a}$$

$$\text{II-a}:\ \mathit{min}\ (c_3\,c_5) > 0,\ \text{II-b}:\ \mathit{min}\ (c_5\,c_6) > 0,$$
$$\text{II-c}:\ \mathit{min}\ (c_1\,c_5) > 0 \tag{60b}$$

$$\begin{aligned} &\text{III-a}: \bar{c}_6,\ \underline{c}_5,\ \bar{c}_4,\ \bar{c}_3,\ \underline{c}_2,\ \underline{c}_1,\ \bar{c}_0 \\ &\text{III-b}: \underline{c}_6,\ \bar{c}_5,\ \underline{c}_4,\ \underline{c}_3,\ \bar{c}_2,\ \bar{c}_1,\ \underline{c}_0 \\ &\text{III-c}: \underline{c}_6,\ \bar{c}_5,\ \bar{c}_4,\ \underline{c}_3,\ \underline{c}_2,\ \bar{c}_1,\ \bar{c}_0 \\ &\text{III-d}: \bar{c}_6,\ \underline{c}_5,\ \bar{c}_4,\ \bar{c}_3,\ \underline{c}_2,\ \underline{c}_1,\ \underline{c}_0 \\ &\textit{are substituted into III, respectively.} \end{aligned} \tag{60c}$$

where $\underline{c}_i$ and $\bar{c}_i$ are the lower and the upper bounds of each c_i, for $i = 1, 2, \ldots, 6$, and

$$\text{III}:\ -\left(4\,c_1\,c_5\,A^2 + 2\,c_3\,A\,B + B^2\right) > 0 \tag{61}$$

where

$$A \equiv c_1\,c_5\,c_6 - c_2\,c_5^2 + c_3\,c_4\,c_5 - c_3^2\,c_6 \tag{62a}$$

$$B \equiv 2\,c_0\,c_5^3 - 2\,c_1\,c_4\,c_5^2 + 2\,c_1\,c_3\,c_5\,c_6 \tag{62b}$$

■

The proof and detail about Corollary 1 can be found in Refs. [4] and [5].

The optimal weighting and length of receding-horizon step-time are determined using the same procedure as the spacecraft attitude maneuver problem in Ref. [5]. The design goal is to determine w_p and/or r_p and h that minimizes the ∞-norm of sensitivity function for the system inside the stable region, which is found using Corollary 1.

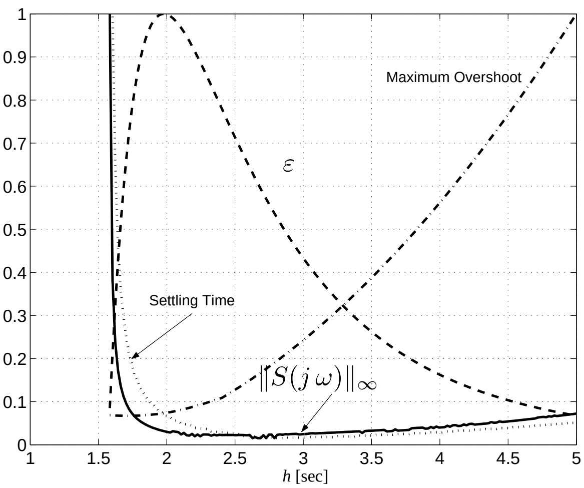

Fig. 6 h vs. ε, $\|S(j\omega)\|_\infty$, Settling Time, and Maximum Overshoot

For this case the stability index and the norm are more sensitive to h than r_p as the one for the case of spacecraft attitude maneuvers in Ref. [5]. Figure 6 depicts h versus the normalized values of $\|S(j\omega)\|_\infty$, ε, settling time and maximum overshoot for an impulse $\hat{u}(t)$ input, with r_p set to 1 (chosen by trial and error). To minimize the sensitivity norm ($\|S(j\omega)\|_\infty$) the value of h has to be chosen between 2 sec and 3 sec. The optimal value of h is chosen to be 2.5 sec by trial and error. Finally, the determined model-error is given by

$$\begin{aligned}\hat{\nu}(t) &= 3.69\,\hat{\phi}_1(t) + 0.41\,\hat{\phi}_2(t) \\ &\quad + 0.96\,\hat{\nu}(t-\tau) - 0.16\,\tilde{\alpha}(t)\end{aligned} \tag{63}$$

STABILITY ANALYSIS

The output is selected as the pitch angle, $\hat{\alpha}(t)$, as follows:[9]

$$\hat{y}(t) = \hat{\alpha}(t) \tag{64}$$

The model-error with Padé approximation for the time delay is given by

$$\begin{aligned}\hat{\nu}(t) &= \frac{d(s)}{d(s) + a_3\,n(s)} \\ &\quad \times \left\{\begin{bmatrix} a_1 + a_4, & a_2, & 0, & 0\end{bmatrix} \hat{\boldsymbol{\phi}}(t) + a_4\,v_\alpha(t)\right\}\end{aligned} \tag{65}$$

where $n(s)/d(s)$ is a Padé (4, 4) approximation of the time delay. We now obtain the following:

$$\begin{aligned}\dot{\hat{\boldsymbol{\phi}}}(t) &= \left[A_e - B_e\,D_z\,\mathbf{a}^T\right]\hat{\boldsymbol{\phi}} - B_e\,C_z\,\mathbf{z}(t) \\ &\quad + G_e\,\hat{\mathbf{u}}(t) - B_e\,D_z\,a_4\,v(t)\end{aligned} \tag{66}$$

where each matrix is given by

$$A_e = \begin{bmatrix} 0 & 1 & 0 & 0 \\ -4.0 & -1.2 & 0 & 0 \\ 0 & 0.0054 & 0 & -1.33 \\ 8.63 & -0.23 & 185.6 & -3.58 \end{bmatrix} \tag{67a}$$

$$B_e = \begin{Bmatrix} 0 & 1 & 0 & 0 \end{Bmatrix}^T \tag{67b}$$

$$G_e = \begin{bmatrix} 0_{1\times 3} \\ I_{3\times 3} \end{bmatrix} \tag{67c}$$

In addition each matrix for Eq. (27) is given by

$$E_f = \begin{bmatrix} 0_{1\times 3} \\ I_{3\times 3} \\ 0_{4\times 3} \end{bmatrix} \tag{68a}$$

$$N_f = \begin{bmatrix} 0.2 \times I_{4\times 4} & 0_{4\times 4} \end{bmatrix} \tag{68b}$$

$$Q_q = \begin{bmatrix} I_{4\times 4} & 0_{4\times 4} \\ 0_{4\times 4} & 0_{4\times 4} \end{bmatrix} \tag{68c}$$

The ∞-norm of Eq. (27) with respect to ϵ is shown in Fig. 7. The maximum value of ϵ satisfying the norm less than 1 is 0.0492.

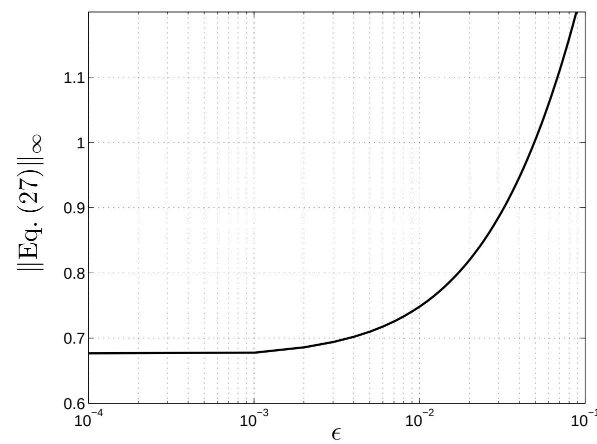

Fig. 7 ∞-norm Condition for the Quadratic Stability with Respect to ϵ

SIMULATION

The simulation parameters are given in Table 1 with $b = 0.135$ m, $a = -0.6847$ and $U = 13$ m/sec. The nonlinear spring constant, k_α, is given by Eq. (31). The nominal values of the three uncertainty parameters are given by: $\hat{a} = -0.6$, $\hat{U} = 16$ m/sec, and $\hat{k}_\alpha = 6.833$. The initial condition for the plunge displacement, $\mathfrak{h}$, is equal to 0.2 m. To show the capability of the design controller to compensate limit cycle oscillations, the controller is activated at 1 sec after the open-loop response falls into a limit cycle oscillation.[9]

The results are shown in Figs. 8 and 9. As shown in the figures, without MECS the nominal controller fails to stabilize the response. However, with MECS the limit cycle oscillation is stabilized. Also, as shown in the flap deflection history, Fig. 9, the flap deflection is inside the constraints.

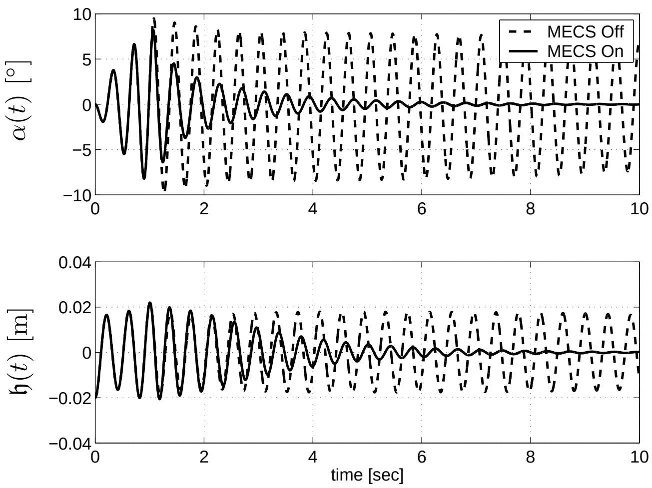

Fig. 8 Time Histories of $\alpha(t)$ and $\mathfrak{h}(t)$ for Each Case

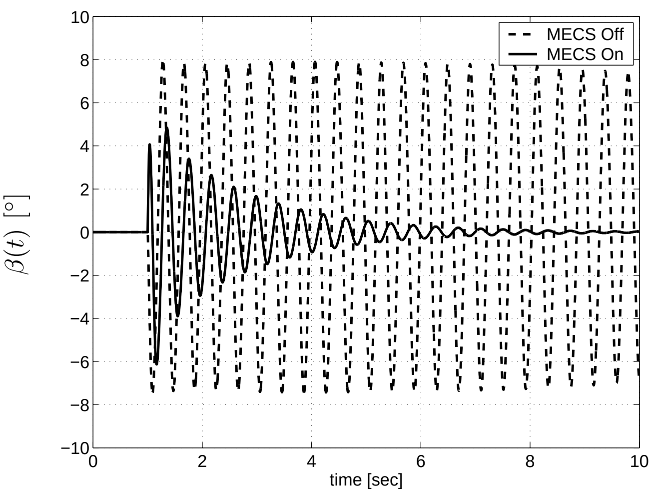

Fig. 9 Time History of $\beta(t)$ for Each Case

CONCLUSION

The modelling errors in the aeroelastic system were determined using a modified approximate receding-horizon expression with a Taylor series expansion at each instant of time. This approach was used in the model-error control synthesis design to provide robustness with respect to the bounded modelling errors. A Predictive filter was designed to estimate the angular velocity and the linear velocity, which were subsequently used in the overall controller, and the estimated velocities were compared to the ones from RTS smoother. Simulation results indicated that a nominal controller combined with the model-error control synthesis approach produced the ability to compensate the limit cycle oscillation. In addition the closed-loop system is globally quadratically stable for a norm bounded nonlinear uncertainty.

ACKNOWLEDGEMENT

The authors would like to thank Dr. T. Strganac, Department of Aerospace Engineering, Texas A&M University at College Station, TX, for allowing us to use the experimental data.

REFERENCES

[1]Crassidis, J. L., "Robust Control of Nonlinear Systems Using Model-Error Control Synthesis," *Journal of Guidance, Control, and Dynamics*, Vol. 22, No. 4, July-August 1999, pp. 595–601.

[2]Crassidis, J. L. and Markley, F. L., "Predictive Filtering for Nonlinear Systems," *Journal of Guidance, Control, and Dynamics*, Vol. 20, No. 3, May-June 1997, pp. 566–572.

[3]Kim, J. and Crassidis, J. L., "Linear Stability Analysis of Model-Error Control Synthesis," *AIAA GN&C Conference & Exhibit*, Denver, CO, 2000, Aug. 14-16, AIAA-2000-3963.

[4]Kim, J. and Crassidis, J. L., "Model-Error Control Synthesis Using Approximate Receding-Horizon Control Laws," *AIAA GN&C Conference & Exhibit*, Montreal, QB, Canada, 2001, Aug. 6-9, AIAA-2001-4220.

[5]Kim, J. and Crassidis, J. L., "Robust Spacecraft Attitude Control Using Model-Error Control Synthesis," *AIAA GN&C Conference & Exhibit*, Monterey, CA, 2002, Aug. 5-8, AIAA-2002-4576.

[6]Lu, P., "Approximate Nonlinear Receding-Horizon Control Laws in Closed Form," *International Journal of Control*, Vol. 71, No. 1, 1998, pp. 19–34.

[7]Gantmacher, F. R., *The Theory of Matrices*, Vol. II, Chelsea Publishing Company, 1959.

[8]Kim, J. and Crassidis, J. L., "Fundamental Relation of Approximate Receding-Horizon Optimization to the Simple Mass-Spring-Damper System," *AIAA GN&C Conference & Exhibit*, Austin, TX, 2003, Aug. 11-14, AIAA-2003-5633.

[9]Strganac, T. W., Ko, J., and Thompson, D. E., "Identification and Control of Limit Cycle Oscillations in Aeroelastic Systems," *Journal of Guidance, Control, and Dynamics*, Vol. 23, No. 6, November-December 2000, pp. 1127–1133.

[10]Xue, A., Lin, Y., and Sun, Y., "Quadratic Guaranteed Cost Analysis for a Class of Nonlinear Uncertain Systems," *Proceeings of the 2001 IEEE International Conference on Control Applications*, IEEE, Mexico City, Mexico, September 2001.

[11]Paraskevopoulos, P. N., *Digital Control Systems*, Prentice Hall Europe, 1996.

[12]Gelb, A., *Applied Optimal Estimation*, The MIT Press, 1974.

[13]Maybeck, P. S., *Stochastic Models, Estimation, and Control*, Vol. 2, Navtech Book & Software Store, Arlington, VA, 1994.

APPENDIX A

The definitions of the parameters in Eq. (34) are given by

$$
\begin{aligned}
P_U[\phi_1(t)] &= k_4\, U^2 + q[\phi_1(t)] \\
Q_U[\phi_1(t)] &= k_2\, U^2 + p[\phi_1(t)] \\
A_{32} &= g_3/g_4 \\
A_{34} &= 1/g_4 \\
A_{42} &= -c_1\, g_3 - c_2\, g_4 + c_3\, g_3^2/g_4 + c_4\, g_3 \\
A_{43} &= k_3\, g_3 - k_1\, g_4 \\
A_{44} &= c_3\, g_3/g_4 - c_1 \\
p[\phi_1] &= -m_W\, x_\alpha\, b\, k_\alpha(\phi_1)/d \\
q[\phi_1] &= m_T\, k_\alpha(\phi_1)/d \\
d &= m_T\, I_\alpha - m_W^2\, x_\alpha^2\, b^2
\end{aligned}
$$

where

$$
\begin{aligned}
k_1 &= I_\alpha\, k_h/d \\
k_2 &= \left(I_\alpha\, \rho\, b\, c_{l\alpha} + m_W\, x_\alpha\, \rho\, b^3\, c_{m\alpha}\right)/d \\
k_3 &= -m_W\, x_\alpha\, b\, k_h/d \\
k_4 &= -\left(m_W\, x_\alpha\, \rho\, b^2\, c_{l\alpha} + m_T\, \rho\, b^2\, c_{m\alpha}\right)/d \\
c_1 &= \left[I_\alpha\, (c_h + \rho\, U\, b\, c_{l\alpha}) + m_W\, x_\alpha\, \rho\, U\, b^3\, c_{m\alpha}\right]/d \\
c_2 &= \left\{\left[I_\alpha\, \rho\, U\, b^2\, c_{l\alpha} + m_W\, x_\alpha\, \rho\, U\, b^4\, c_{m\alpha}\right] \left(\frac{1}{2} - a\right) \right. \\
&\quad \left. - m_W\, x_\alpha\, b\, c_{l\alpha}\right\}/d \\
c_3 &= \left[-m_W\, x_\alpha\, b\, (c_h + \rho\, U\, b\, c_{l\alpha}) - m_T\, \rho\, U\, b^2\, c_{m\alpha}\right]/d \\
c_4 &= \left\{\left[m_T\, c_\alpha - \left(m_T\, \rho\, U\, b^3\, c_{m\alpha} + m_W\, x_\alpha\, \rho\, U\, b^3\, c_{l\alpha}\right) \right.\right. \\
&\quad \left.\left. \left(\frac{1}{2} - a\right)\right]\right\}/d \\
g_3 &= -\left(I_\alpha\, \rho\, b\, c_{l\beta} + m_W\, x_\alpha\, b^3\, \rho\, c_{m\beta}\right)/d \\
g_4 &= \left(m_W\, x_\alpha\, \rho\, b^2\, c_{l\beta} + m_T\, \rho\, b^2\, c_{m\beta}\right)/d
\end{aligned}
$$

Each matrix in Eq. (47) is given by

$$
\hat{A} \equiv \begin{bmatrix}
0 & 1 & 0 & 0 \\
-121.0 - 0.156\,\hat{U}^2 & -0.299 - 0.032\,\hat{U} & 447.0 & 10.6 + 0.383\,\hat{U} \\
0 & 0.078 & -2.46 & 0.0 \\
-4.26 + 0.021\,\hat{U}^2 & -0.339 + 0.004\,\hat{U} & 109.1 & -2.59 - 0.053\,\hat{U}
\end{bmatrix}
$$

$$
\hat{B} \equiv \begin{Bmatrix} 0 \\ -0.406\,\hat{U}^2 \\ 0 \\ 0 \end{Bmatrix}, \quad \hat{G}_s \equiv \begin{bmatrix} 0 & 0 \\ 1 & 0 \\ 0 & 0 \\ 0 & 1 \end{bmatrix}
$$

$$
\hat{\mathbf{u}}_s(t) \equiv \begin{bmatrix} \hat{u}_1(t) & \hat{u}_3(t) \end{bmatrix}^T
$$

Each matrix in Eq. (50) is given by

$$
\hat{A}_d \equiv \begin{bmatrix}
0.97 & 0.0016 & -0.0004 & 0.0000 \\
-29.0 & 0.62 & -0.26 & 0.0079 \\
0.0012 & 0.0001 & 0.92 & -0.0023 \\
-1.24 & 0.011 & 26.40 & 0.14
\end{bmatrix}
$$

$$
\hat{B}_d \equiv \begin{Bmatrix} 0.0001 \\ 0.0516 \\ 0 \\ 0 \end{Bmatrix}, \quad G_{y_k} \equiv \begin{bmatrix} 0.0315 & 0.0001 \\ 29.1819 & 0.0458 \\ -0.0011 & 0.0848 \\ 1.2421 & -26.4543 \end{bmatrix}
$$

APPENDIX B

For the following simple mass-spring-damper system

$$
\ddot{\hat{x}}(t) + 2\,\zeta\,\omega_n\,\dot{\hat{x}}(t) + \omega_n^2\,\hat{x}(t) = u(t) + \hat{u}(t)
$$

For $N = 2$, the coefficients of the MARH approach are as follows:

$$
\hat{u}(t) = a_1\,\hat{x}(t) + a_2\,\dot{\hat{x}}(t) + a_3\,u(t) + a_4\,\tilde{y}(t)
$$

where

$$
\begin{aligned}
a_1 &= \left\{\omega_n^6 \left(h^2 + \frac{4\,\zeta}{\omega_n}\,h - \frac{6}{\omega_n^2}\right) \left(h^4 + \frac{4\,\zeta}{\omega_n}\,h^3 \right.\right. \\
&\quad \left. - \frac{8}{\omega_n^2}\,h^2 + \frac{4}{\omega_n^4}\right) w_1\,r_1\,r_2 + h^4\,(\,h - 2\,)\,r_2 \\
&\quad - \frac{h^5}{16}\left[\left(\omega_n^2 - 1\right)\,h + 4\,\zeta\,\omega_n - 2\right] \\
&\quad \left.\left(h^4 + 2\,h^3 - 8\,h^2 + 4\right)\right\}/\left(\,h^2\,a_d\,\right) \\
a_2 &= \left\{2\,\omega_n^4\,\left(\zeta\,\omega_n\,h - 1\right) \left(h^2 + \frac{4\,\zeta}{\omega_n}\,h - \frac{6}{\omega_n^2}\right) \right. \\
&\quad \left(h^2 + \frac{4\,\zeta}{\omega_n}\,h - \frac{4}{\omega_n^2}\right) w_1\,r_1\,r_2 + h^4\,(\,h - 2\,)\,r_2 \\
&\quad - \frac{h^5}{16}\left[\left(\omega_n^2 - 1\right)\,h + 4\,\zeta\,\omega_n - 2\right] \\
&\quad \left.(h - 2)\,\left(h^2 + 2\,h - 4\right)\right\}/\left(\,h\,a_d\,\right) \\
a_3 &= \left\{-\omega_n^4\,\left(h^2 + \frac{4\,\zeta}{\omega_n}\,h - \frac{6}{\omega_n^2}\right) \right. \\
&\quad \left(h^2 + \frac{4\,\zeta}{\omega_n}\,h - \frac{8}{\omega_n^2}\right) w_1\,r_1\,r_2 \\
&\quad - h^4\,r_2 + \frac{h^5}{16}\left[\left(\omega_n^2 - 1\right)\,h + 4\,\zeta\,\omega_n - 2\right] \\
&\quad \left.(h - 2)\,(h + 4)\right\}/a_d \\
a_4 &= \left\{-4\,\omega_n^2\,\left(h^2 + \frac{4\,\zeta}{\omega_n}\,h - \frac{6}{\omega_n^2}\right) w_1\,r_1\,r_2 + 2\,h^4\,r_2 \right. \\
&\quad \left. + \frac{h^5}{4}\left[\left(\omega_n^2 - 1\right)\,h + 4\,\zeta\,\omega_n - 2\right]\right\}/\left(\,h^2\,a_d\,\right)
\end{aligned}
$$

and

$$
\begin{aligned}
a_d &= \omega_n^4\,\left(h^2 + \frac{4\,\zeta}{\omega_n}\,h - \frac{6}{\omega_n^2}\right)^2 w_1\,r_1\,r_2 \\
&\quad + \left(h^4 + w_0\,r_1\right)r_2
\end{aligned}
$$